Society For Biomaterials

In vitro evaluation of photo-crosslinkable chitosan-lactide hydrogels for bone tissue engineering

Sungwoo Kim,[1] Yunqing Kang,[1] Ángel E. Mercado-Pagán,[1] William J. Maloney,[1] Yunzhi Yang[1,2]

[1]Department of Orthopedic Surgery, Stanford University, Stanford, California
[2]Department of Materials Science and Engineering, Stanford University, Stanford, California

Received 12 July 2013; revised 4 January 2014; accepted 11 January 2014
Published online 6 February 2014 in Wiley Online Library (wileyonlinelibrary.com). DOI: 10.1002/jbm.b.33118

Abstract: Here we report the development and characterization of novel photo-crosslinkable chitosan-lactide (Ch-LA) hydrogels for bone tissue engineering. We synthesized the hydrogels based on Ch, LA, and methacrylic anhydride (MA), and examined their chemical structures, degradation rates, compressive moduli, and protein release kinetics. We also evaluated the cytotoxicity of the hydrogels and delivery efficacy of bone morphogenetic protein-2 (BMP-2) on osteoblast differentiation and mineralization using W-20-17 preosteoblast mouse bone marrow stromal cells and C2C12 mouse myoblast cells. NMR and FTIR revealed that the hydrogels were formed via amidation and esterification between Ch and LA, and methacrylation for photo-crosslinkable networks. Addition of a hydrophobic LA moiety to a hydrophilic Ch chain increased swellability, softness, and degradation rate of the photo-crosslinkable Ch-LA hydrogels. Changes in Ch/LA ratio and UV exposure time significantly affected compressive modulus and protein release kinetics. The photo-crosslinkable Ch-LA hydrogels were not cytotoxic regardless of the composition and UV crosslinking time. Higher alkaline phosphatase activities of both W-20-17 and C2C12 cells were observed in the less-crosslinked hydrogels at day 5. Mineralization was enhanced by sustained BMP-2 release from the hydrogels, but was cell type dependent. This photo-crosslinkable Ch-LA hydrogel is a promising carrier for growth factors. © 2014 Wiley Periodicals, Inc. J Biomed Mater Res Part B: Appl Biomater, 102B: 1393–1406, 2014.

Key Words: chitosan, lactide, methacrylic anhydride, BMP-2, photo-crosslinkable hydrogel, osteoblastic differentiation, W-20-17, C2C12

How to cite this article: Kim S, Kang Y, Mercado-Pagán ÁE, Maloney WJ, Yang Y. 2014. *In vitro* evaluation of photo-crosslinkable chitosan-lactide hydrogels for bone tissue engineering. J Biomed Mater Res Part B 2014:102B:1393–1406.

INTRODUCTION

In tissue engineering and regenerative medicine, hydrogels have been extensively studied as a means of delivery of growth factors to regulate cell functions as well as enhancing tissue regeneration.[1,2] The ideal hydrogel based delivery system for bone regeneration should have the following characteristics: (1) being able to fill and remain in the cavity of the defect with suitable swelling behavior and mechanical properties, (2) spatial-temporal presentation of bioagents to facilitate and guide migration, proliferation, and differentiation of cells, and (3) gradual degradation corresponding to the rate of tissue regeneration for seamless tissue integration and potential function restoration.[2,3] It is well known that chemistry, network structure, and reaction mechanisms of hydrogels determine hydrogel properties and its delivery kinetics.

Recently, photo-crosslinkable hydrogels have been intensively studied in many biomedical applications such as drug delivery,[3–5] cell therapy,[6] and tissue engineering scaffolds.[7] The agents delivered including drugs, growth factors, and cells are loaded into an injectable formula, that can be directly applied to the targets in a minimally invasive manner. The crosslinking of the hydrogel occurs covalently and irreversibly *in situ* via UV light irradiation. The photo-crosslinking method can avoid uncontrollable and inconsistent gel formation due to the reactions that occur immediately by mixing with crosslinkers.[4,7] The precise structure of the crosslinked hydrogel networks can be also achieved by photolithography or rapid prototyping (RP) techniques.[6]

In addition, hydrogels and polymers resembling extracellular matrix (ECM) are of great interest for growth factor delivery because they possess ECM-like chemistry, structure, physicochemical, and mechanical properties that potentially benefit storage and controlled release of growth factors.[2,8] For example, among polysaccharides, chitosan (Ch) has been

Additional Supporting Information may be found in the online version of this article.
Correspondence to: Y. P. Yang (e-mail: ypyang@stanford.edu)
Contract grant sponsor: DOD PRORP; contract grant number: W81XWH-10-1-0966
Contract grant sponsor: Airlift Research Foundation; contract grant number: W81XWH-10–200-10
Contract grant sponsor: Wallace H. Coulter Foundation
Contract grant sponsor: NIH from NIAMS; contract grant number: R01AR057837
Contract grant sponsor: NIH from NIDCR; contract grant number: R01DE021468

studied for drug delivery, wound healing, and tissue regeneration due to the presence of amino groups, providing a great opportunity for chemical modification and beneficial biological properties such as biocompatibility and biodegradability.[9–13] In addition, polylactide (PLA) has been also widely used for sustained drug delivery systems and orthopedic devices.[11–14] However, the high crystallinity and hydrophobicity of PLA cause slow degradation rate and low cell adhesion, limiting its application for tissue regeneration. Methacrylic anhydride (MA) has been commonly used in the preparation of crosslinkable polymer networks such as Ch-MA due to the high reactivity of methacrylic double bonds.[14,15] Though Ch-PLA copolymers have been studied for tissue engineering or drug delivery in the form of film, scaffolds, or nanoparticles,[11–13] as well as Ch-MA based biomaterials,[15–17] to our best knowledge, Ch-lactide (LA) based photo-crosslinkable hydrogels have not been reported.

Herein, we report the development and characterization of novel photo-crosslinkable Ch-LA hydrogels with tunable swelling behaviors, degradation rates, mechanical properties, and protein release kinetics. We hypothesized that the Ch-LA hydrogel would combine excellent biocompatibility, protein affinity, and degradability from Ch, and tunable physical and mechanical properties from LA.[1] We also hypothesized that crosslinking density by methacrylation would further regulate the physicochemical properties of hydrogels. We rationalized that hydrophilic Ch backbone molecules and hydrophobic PLA side chains can form the hydrophobic–hydrophilic copolymer network, providing the flexibility of the hydrogel, while MA incorporation can form different crosslinking density via photo-initiation of its highly reactive double bonds.[14] The former is determined by the Ch-LA ratio or the amount of LA, and the distribution of the hydrophobic molecules along the backbone [14]. The latter is determined by the concentration of MA, UV radiation intensity, and crosslinking time.[15,16] As a result, the manipulation of these parameters regulates the network structure, protein affinity, and physicochemical properties of hydrogels, which affect swelling behavior, degradation rate as well as protein release kinetics of the hydrogels.

To test our hypotheses, in the present study, we first synthesized the photo-crosslinkable Ch-LA copolymer using Ch, LA, and MA. Then, we examined degradation rates, compressive modulus, and protein release kinetics of the photo-crosslinkable Ch-LA hydrogels. In addition, we investigated the cytotoxicity and efficacy of the delivery system by measuring *in vitro* bioactivity of BMP-2 using W-20-17 preosteoblast mouse bone marrow stromal cells and C2C12 mouse myoblast cells. Our results have showed that a novel photo-crosslinkable, biodegradable Ch-LA hydrogel was successfully synthesized and used to effectively deliver growth factor to regulate cell response *in vitro*.

MATERIALS AND METHODS

Materials

Ch ($\geq$ 310 kDa, 75% or greater degree of deacetylation) and MA were purchased from Sigma-Aldrich (St Louis, MO). D,L-Lactide was purchased from Ortec (Piedmont, SC). Human bone morphogenetic protein-2 (BMP-2) was obtained from Medtronic (Minneapolis, MN). All other chemicals were reagent grade and were used as received. An UV light source (Omnicure S2000) was purchased from Lumen Dynamics Group Inc (Ontario, Canada).

Synthesis of photo-crosslinkable hydrogels

A 1% (wt/vol) Ch solution was prepared by stirring powdered Ch in 0.75% (vol/vol) aqueous acetic acid at room temperature overnight. The insoluble particles in the Ch solution were removed by filtration. An aqueous solution of lactic acid was prepared by dissolving powdered D,L-lactide in DMSO (dimethyl sulfoxide) at 80°C. Different mass ratios of Ch to LA were prepared (8:1, 4:1, or 1:1). The mixture of Ch and LA was stirred using a magnet stirrer for 1 h at 80°C. Tin (II) 2-ethylhexanoate and triethylamine (TEA) were added dropwise. The mixture was reacted at 80°C with magnetic stirring for 20 h in nitrogen atmosphere. The mixture was dialyzed in distilled water using dialysis tubing (molecular weight cut off: 14,000) for 1 day. 2.5% (wt/vol) MA was added into the dialyzed mixture dropwise, and the reaction continued for 8 h at 60°C. Similarly, for Ch hydrogels (Ch), 2.5% (wt/vol) MA was added into the Ch solution dropwise, and the reaction continued for 8 h at 60°C. After the reaction, the mixture was dialyzed in distilled water using dialysis tubing (molecular weight cut off: 14,000) for 7 days. The obtained solution was then freeze-dried for 2–3 days and stored at −20°C until use. For the photo-crosslinkable hydrogel formulation, the freeze-dried samples were reconstituted as a 2% (wt/vol) in distilled water. The photoinitiator (Irgacure 2959, CIBA Chemicals) was completely dissolved into distilled water at 70°C. The photoinitiator solution was sterile-filtered through a 0.22-μm filter and then added to the prepolymer solutions to make a final concentration of 0.5% (wt/vol). The prepolymer solutions were then exposed to 6.9 mW/cm^2 UV light to allow for free radical polymerization by photo-crosslinking. As shown in Scheme 1, the Ch/LA hydrogels were prepared by reacting D,L-lactide with Ch at different mass ratios and varying UV exposure times.

Characterization of hydrogels

Proton nuclear magnetic resonance spectroscopy. The structural characterization of Ch, Ch/LA, and Ch/LA/MA, was performed by NMR spectroscopy. Samples were dissolved and prepared in CD_3COOD for nuclear magnetic resonance (NMR) measurements, and the proton nuclear magnetic resonance (^{1}H-NMR) spectra were obtained on a Varian Inova-300 spectrometer. All the chemical shifts for resonance signals were reported in parts per millions (ppm).

Fourier transform infrared spectroscopy spectra. In order to investigate the chemical structure of prepolymer solutions including Ch, Ch/LA, and Ch/LA/MA, Fourier transform infrared spectroscopy (FTIR) spectra were obtained using a Bruker Vertex 70 FTIR spectrometer coupled to a PC with analysis software. Samples were placed in the

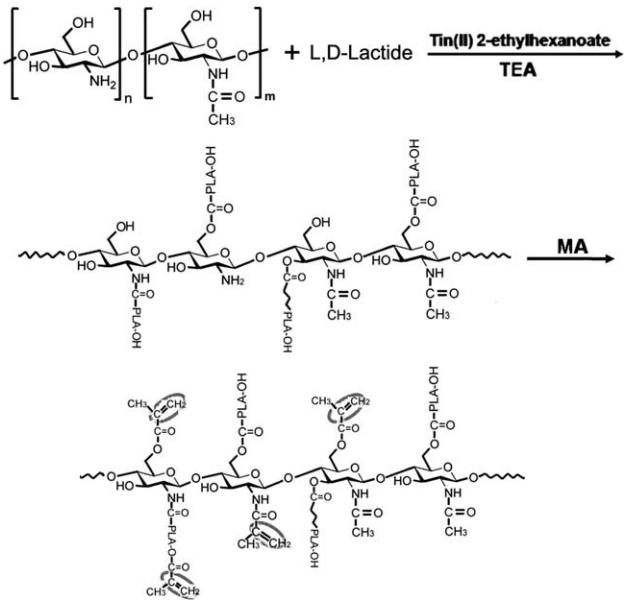

SCHEME 1. Synthesis scheme of Ch and LA copolymer and methacrylation of the copolymer.

holder directly in the IR laser beam. All spectra were recorded in transmittance mode (40 times scanning, 800–4000 cm^{-1}).

Scanning electron microscopy. The internal microstructures of the hydrogels were investigated by comparing Ch with Ch/LA (1:1) hydrogels. The effect of UV crosslinking times (30 s and 300 s) on the morphological change of the hydrogels was also observed. The hydrogel samples were incubated into phosphate buffered saline (PBS) (pH 7.4) at 37°C for 1 day and lyophilized overnight (Freezone, LABCONCO). The samples were sputter-coated with gold and examined under a scanning electron microscope (Hitachi S-3400N VP SEM) operated at a 10 kV voltage. Porosity was calculated from scanning electron microscopy (SEM) images by utilizing NIH ImageJ software to determine pore size in a viewing field.

Mechanical testing

Unconfined compression tests were performed to determine the effect of introduction of LA to Ch and UV crosslinking times on the mechanical properties of the hydrogels using an Instron 5944 materials testing system (Instron Corporation, Norwood, MA) fitted with a 10 N load cell (Interface Inc., Scottsdale, AZ). The prepolymer solution was pipetted into a cylindrical Teflon mold and exposed to 6.9 mW/cm^2 UV light. The diameter (~6 mm) and thickness (~3 mm) of the samples were measured using digital calipers and the material testing system's position read-out, respectively. Before each test, a preload of approximately 2 mN was applied. The upper platen was then lowered at a rate of 1% strain/s to a maximum strain of 30%. Load and displacement data were recorded at 100 Hz. The compressive modulus was determined for strain ranges of 10–20% from linear curve fits of the stress–strain curve in each strain range. All tests were conducted in PBS solution at room temperature.

In vitro degradation characteristics

In vitro degradation of the hydrogels was investigated according to different ratios of Ch to LA and UV exposure times. The swelling behavior or degradation profile of the hydrogels was determined by measuring the wet weight remaining ratio of the hydrogels in both PBS (pH 7.4) and lysozyme containing PBS.[18] In order to accelerate the degradation process *in vitro*, we used a higher concentration of lysozyme than the physiological concentration found in serum (1.5 μg/mL).[19] The hydrogels were surface dried and weighed (W_0). Then the hydrogels were placed into PBS (pH 7.4) or 100 μg/mL lysozyme/PBS solution at 37°C. At designated time points over a period of 15 days, the samples were taken out and weighed again (W_1) every other day. The wet weight remaining ratio was calculated as follows: Wet weight remaining ratio (%) = $W_1/W_0 \times 100\%$.

In vitro release study

To study the release kinetics of the protein from the hydrogels, bovine serum albumin (BSA) was used as a model protein. This study evaluated the release kinetics of BSA from the hydrogel according to different ratios of Ch to LA and UV crosslinking times. BSA was mixed with prepolymer solution to form a homogenous solution, and then was preserved at 4°C overnight prior to the experiment. Approximately 80 μg/mL of BSA was loaded. The mixture was then pipetted into a cylindrical Teflon mold and exposed to 6.9 mW/cm^2 UV light. The hydrogels with diameter of 6 mm and thickness of 3 mm were prepared. Each sample was placed in a container containing 3 mL of PBS (pH 7.4) and incubated at 37°C for 15 days. At designated time points, 500 μL aliquots of the release medium were sampled and the same amount of fresh PBS (pH 7.4) was added into each container. In the collected fractions, the cumulative release amounts of BSA from the hydrogels were determined as a function of time by bicinchoninic acid (BCA) assay (Pierce, Rockford, IL). The optical density of each sample was determined using a microplate reader at 560 nm (TECAN Infinite F50).

In vitro bioactivities

Cell culture. Two different cell lines, the W-20-17 preosteoblast mouse bone marrow stromal cells and C2C12 mouse myoblast cells, were purchased from ATCC (Manassas, VA). They were grown and maintained in Dulbecco's modified Eagle's medium (DMEM) media with 10% FBS, 1% antibiotic/antimycotic mixture, 5 mL of L-glutamine (200 m*M*), and sodium pyruvate. The cells were cultured in an incubator supplied with 5% CO_2 at 37°C. The culture medium was changed every 3 days.

Cytotoxicity of hydrogels,. The cytotoxicity of the hydrogels was examined via an indirect cell culture. The cells were seeded in the bottom of 12-well plates at a density of 60,000 cells/well and the hydrogels were placed into the

cell culture inserts (BD BioCoat™ Control Cell Culture inserts). After incubation for 1 and 3 days, the number of viable cells was determined quantitatively using a CellTiter 96® AQueous One Solution (MTS) assay according to the manufacturer's instructions. The light absorbance at 490 nm was recorded using a micro plate reader (TECAN Infinite F50). Before the assay, the cellular morphology was observed using a Zeiss Axiovert 200 microscope (Carl Zeiss Microimaging, Thornwood, NY). Photomicrographs of cells were processed using imaging software (Zeiss, AxioVision).

Alkaline phosphatase activity of cells in response to BMP-2. We investigated the effect of BMP-2 released from the hydrogels on alkaline phosphatase (ALP) activity of cells. In this study, two different cell lines were used. The W-20-17 cell line has been used under the ASTM F2131 standard to evaluate activity of BMP-2 *in vitro*. The C2C12 cell line was also selected because they shift in the differentiation pathway from myoblastic to osteoblastic after treatment with BMP-2. Cells were seeded in 24-well plates at a density of 60,000 cells/well and incubated for 5 days. Two control groups did not contain the hydrogels. In the negative control group, cells were incubated in DMEM without BMP-2. In the positive control group, 100 ng/mL of BMP-2 was added into the culture medium on day 1, but it was not replenished after changing medium at day 3. In the experimental group, cells were cultured in the DMEM media containing the Ch/LA (8:1) hydrogels made by different UV exposure times (30 s and 300 s). The Ch/LA (8:1) hydrogels loaded with BMP-2 (100 ng/mL) were placed into the plates on day 1. The positive control group was designed for a burst release effect of BMP-2. The experimental gel group was designed for a sustained release effect of BMP-2. After incubating for 5 days, the medium was removed from cell culture and the cell layers were washed in PBS (pH 7.4) once. ALP activity was detected using Sigma-Aldrich Alkaline Phosphatase kits according to the manufacturer's instructions (Sigma-Aldrich, St. Louis, MO). Histochemical semi-quantitative imaging of ALP was obtained using a Zeiss Axiovert 200 microscope (Carl Zeiss Microimaging, Thornwood, NY). Quantification of the staining was performed using Adobe Photoshop 7.0 (Adobe Systems, San Jose, CA). The image histogram tool was used to measure average pixel intensity.

Alizarin Red S staining for calcium mineralization. Calcium mineral content within the cell layers was determined qualitatively and quantitatively by Alizarin Red S staining (AR-S). Cells were seeded in 24-well plates at a density of 30,000 cells/well and incubated in DMEM for 1 day, and then the culture medium was changed to osteogenic media containing 10% FBS, 10 m*M* β-glycerophosphate, 10 n*M* dexamethasone, and 50 mg/mL ascorbic acid. Two control groups did not contain the hydrogels as described in section "Alkaline phosphatase activity of cells in response to BMP-2." In the negative control group, cells were incubated in osteogenic medium without BMP-2. In the positive control group, 100 ng/mL of BMP-2 was added into the osteogenic medium on day 1, but was not replenished after changing medium at day 3. In the experimental group, the Ch/LA (8:1) hydrogels, that were made by different UV exposure times (30 s and 300 s), were loaded with BMP-2 (100 ng/mL) and placed into the plates on day 1. The positive control group was designed for a burst release effect of BMP-2. The experimental gel group was designated for a sustained release effect of BMP-2. At each time point (10 and 21days of incubation), the cell layers were washed with PBS (pH 7.4) twice and fixed in ice-cold 50% ethanol at 4°C for 30 min. After washing with distilled water, they were dried at room temperature and stained by adding 1 mL of 1% Alizarin Red S (10 mg/mL) at room temperature for 45 min. The cell layers were then washed with distilled water five times and dried. Stained cell layers were photographed using a Zeiss Axiovert 200 microscope (Carl Zeiss Microimaging, Thornwood, NY). Quantitative calcium mineral contents were measured by a destaining procedure using an extraction solvent containing a mixture of 10% acetic acid and methanol at room temperature for 30 min. About 200 μL aliquots of Alizarin Red S extracts were then added in a 96-well assay plate. The Alizarin Red S concentrations of the samples and standard were determined at an absorbance of 405 nm and expressed as μg/mL.

Statistical analysis

All data are presented as mean ± standard deviation. Significant differences were analyzed by one-way ANOVA test. The differences in groups and experimental time points at any time were considered significant if $p < 0.05$.

RESULTS

Characterization of Ch/LA hydrogels

Proton nuclear magnetic resonance spectroscopy. Figure 1 shows ^{1}H-NMR spectra of Ch, Ch/LA, and Ch/LA/MA. The characteristic peaks from the samples associated with Ch, lactic acid, and MA segments were assigned according to the data reported in the literature.[11–15,20] Ch showed multiplets at δ 3.26–3.89 due to H-3, H-4, H-5, and 2H-6 in the ring of the glucosamine and the signals at δ 1.80, 2.00, and 2.21 assigned to H-2 of *N*-acetylglucosamine units of chitin.[18] Compared with Ch, the ^{1}H-NMR spectra of Ch/LA not only showed the signals of Ch, but also had new peaks at δ 4.30–4.53 and δ 5.23 assigned to the terminal methine protons of the PLA branches and their repeat units in the chain, respectively.[11–13] The signals at δ 1.48–1.59 and δ 1.31 were attributed to the methyl protons of the PLA located at the terminal groups.[11–13] The results revealed that Ch/LA contained PLA side chains. The spectrum for Ch/LA/MA showed, in addition to the signals assigned in the Ch/LA, the presence of new signals at δ 6.23 and δ 5.74 attributable to the vinyl protons ($C{=}CH_2$) of the methacrylic groups and a singlet at δ 1.97 due to the methyl protons (CH_3) of the methacrylic group.[14,15] The peaks from δ 1.87 to 2.31 corresponded to the methylene carbons of acetyl groups on unmodified regions of Ch and methacrylamide pendents of methacrylated Ch.[14,15] These new spectra indicated the results of esterification and amidation when comparing the ^{1}H-NMR spectrum of the Ch with those of the Ch after modification with LA (Ch/LA) and MA (Ch/LA/MA).

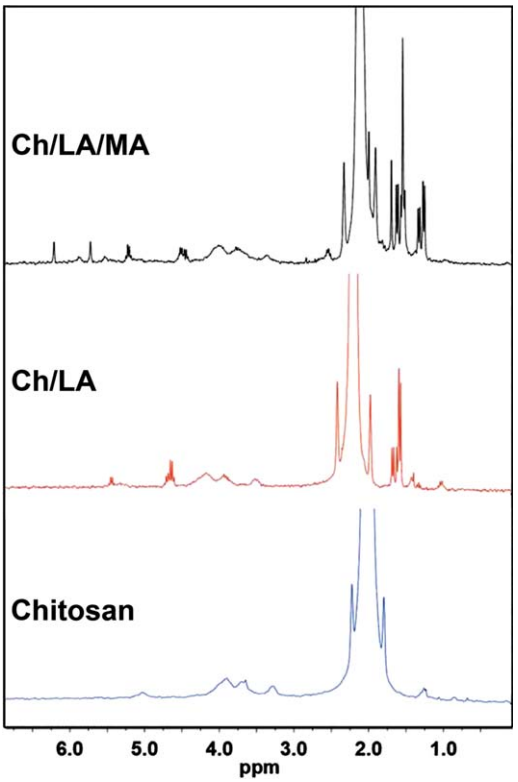

FIGURE 1. The ^{1}H-NMR spectra of Ch, Ch/LA, and Ch/LA/MA. [Color figure can be viewed in the online issue, which is available at wileyonlinelibrary.com.]

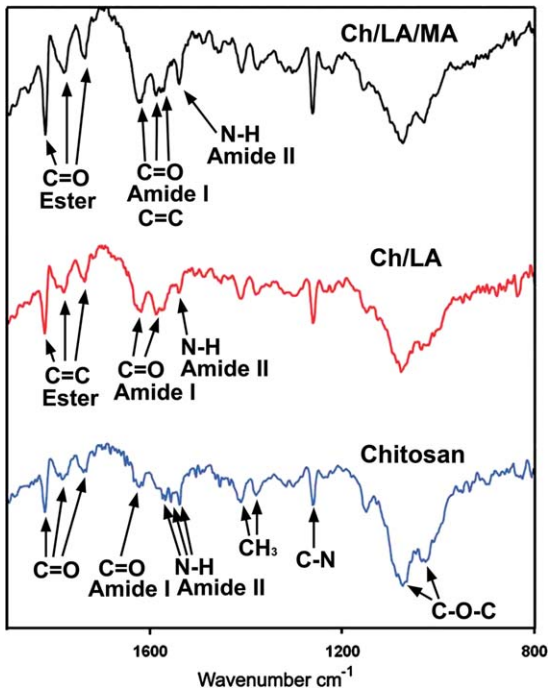

FIGURE 2. FTIR spectra of Ch, Ch/LA, and Ch/LA/MA. [Color figure can be viewed in the online issue, which is available at wileyonlinelibrary.com.]

Fourier transform infrared spectroscopy spectra. Structure changes of the prepolymer solutions were also confirmed by FTIR spectra (Figure 2). The spectrum of the Ch exhibited several characteristic peaks which were attributed to the C═O stretching vibrations of amide I at 1622 cm^{-1}, the N—H bending vibrations of amide II at 1540, 1556, and 1568 cm^{-1}, and the C—N bending of the amine groups at 1261 cm^{-1}. The peaks at 1072 cm^{-1} and 1022 cm^{-1}, representative of the C—O—C bending, were observed. The peaks at 1373 and 1405 cm^{-1} were the characteristic bands of CH_3 symmetrical deformation. The absorption at 1733, 1744, and 1818 cm^{-1} was probably attributed to C═O stretching vibrations of *N*-acetyl groups in the Ch backbone, indicating the Ch was not completely deacetylated.

Compared to the IR spectrum of Ch, the intensity of amide I at 1622 cm^{-1} was enhanced after LA modification (Ch/LA). The peaks ascribed to the N—H bending vibrations of amide II changed and shifted to 1537 and 1577 cm^{-1}, indicating that the amount of amide group increased in the copolymer (Ch/LA) after the reaction. The peaks at 1733, 1774, and 1818 cm^{-1} assigned to C═O stretching vibrations were enhanced owing to the overlapping of the peaks from *N*-acetyl groups in the Ch and the ester that coupled the Ch and LA. This evidence indicates that the carbonyl groups of the LA also interact with hydroxyl groups of the Ch.

When the Ch/LA reacted with MA to form Ch/LA/MA, the increased intensity of the amide I peak (1616 cm^{-1}) and amide II (1539, 1571, and 1579 cm^{-1}) indicated an increase in amidation. In addition, the absorption peaks in the range from 1600 to 1647 cm^{-1}, that were attributed to the C═C stretching vibrations, were overlapped with the peaks from the amide I. The enhanced peaks at 1735, 1776, and 1818 cm^{-1} were assigned to the C═O stretching vibrations due to *N*-acetyl groups in the Ch and the ester that coupled the Ch and MA. This evidenced the reactions between MA with Ch-LA.

SEM observations. Figure 3 shows SEM micrographs of cross-sectional area of freeze-dried hydrogels after incubation in PBS (pH 7.4) at 37°C for 1 day. All hydrogels were highly porous, but displayed distinct morphology between samples throughout the cross-section. Ch alone [Figure 3(a–d)] exhibited a porous structure with smaller pore sizes (94.5 ± 8.31 at 30 s and 82.8 ± 2.43 μm at 300 s of UV exposure time) compared to the combination of Ch with LA [Figure 3(e–h)]. The Ch/LA (1:1) made by UV 30 s exposure exhibited the largest pore size (576.69 ± 24.52 μm) among the four groups of hydrogels, indicating higher swelling behavior after incubation in PBS for 1 day. Similarly, with increasing UV exposure time, the pore size (280.68 ± 30.15 μm) of Ch/LA (1:1) became smaller than that of Ch/LA (1:1) at 30 s of irradiation. It is likely that longer UV exposure on the prepolymer solution produces more crosslinked networks. SEM images demonstrated that these structural properties varied with the composition of the hydrogel and crosslinking density via exposure time.

Mechanical testing

Mechanical properties of the hydrogels were investigated according to different ratios of Ch to LA and UV crosslinking

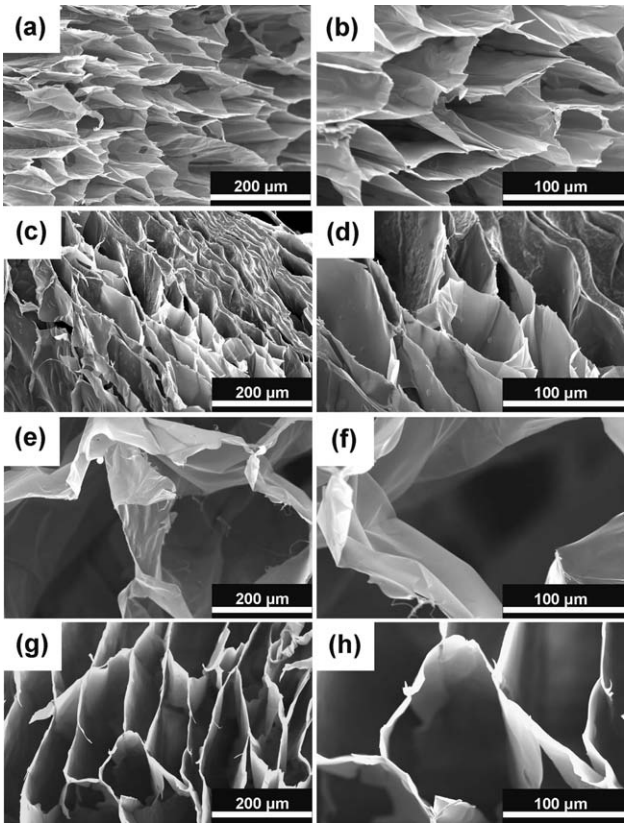

FIGURE 3. Representative SEM micrographs on the cross-section of the freeze-dried Ch hydrogels made by (a,b) 30 s and (c,d) 300 s of UV irradiation; Ch/LA (1:1) hydrogels made by (e, f) 30 s and (g,h) 300 s of UV irradiation. Samples were incubated at 37°C for 1 day and lyophilized overnight before the examination under a scanning electron microscope (Hitachi S-3400N VP SEM) operated at 10 kV voltages. (Bar = 100 or 200 μm).

times (Figure 4). The results showed that the compressive modulus of the hydrogels increased with increasing ratio of Ch to LA. At 30 s of UV light irradiation, Ch alone showed significantly higher compressive modulus than the combinations of Ch and LA ($p < 0.05$). There was also significant difference in the compressive modulus between Ch/LA (8:1) and Ch/LA (1:1) ($p = 0.039$). The compressive modulus of the hydrogels significantly increased with increasing UV crosslinking time in all the groups. Ch possessed 5 ± 0.68, 21.6 ± 2.04, and 35.2 ± 5.1 kPa of compressive modulus at 30 s, 120 s, and 300 s of UV exposure time, respectively. Ch/LA (8:1) showed 4 ± 0.38, 22.4 ± 4.1, and 33.2 ± 2.61 kPa of compressive modulus at 30 s, 120 s, and 300 s, respectively. Ch/LA (4:1) had 1.9 ± 1.11, 14 ± 3.23, and 16.9 ± 3.15 kPa of compressive modulus at 30 s, 120 s, and 300 s, respectively. Ch/LA (1:1) also significantly increased compressive modulus from 1.3 ± 0.48 kPa at 30 s to 15.2 ± 0.86 kPa at 300 s. This indicated that a longer UV crosslinking time increased cross-linking degree, resulting in reinforced microstructure of the hydrogels. However, the compressive modulus of the hydrogels was inversely proportional to the amount of LA in the hydrogel network. The higher ratio of LA displayed lower compressive modulus of the hydrogels compared to the others. This result indicated that mechanical strength was dependent on the ratio of Ch to LA and crosslinking density via UV irradiation. A higher ratio of Ch to LA and a longer exposure time increased stiffness of the hydrogels.

In vitro degradation characteristics of hydrogels

To understand the influence of the different ratios and UV exposure times on the degradation behavior of hydrogels, the wet weight remaining ratio of the hydrogels in PBS (pH 7.4) was examined as shown in Figure 5. The gels were also tested in PBS (pH 7.4) containing lysozyme (100 μg/mL). In PBS, the wet weight remaining ratio of Ch/LA (1:1) at 30 s of UV exposure time significantly increased compared with the other groups at the same UV exposure time ($p < 0.05$). The other groups showed less than 20% decrease in wet weight remaining ratio at all UV exposure times and the shape of the hydrogels was well maintained in PBS during 15 days of the incubation. However, the wet weight remaining ratio of Ch/LA (1:1) showed a similar tendency compared with the others by increasing UV exposure time. This result showed that the hydrogel with greater portion of LA and shorter UV exposure time induces the absorption of a greater amount of water, resulting in a larger degree of swelling.

In 100 μg/mL lysozyme containing PBS solution, the wet weight remaining ratio of the hydrogels in all the groups significantly decreased with time at 30 s UV exposure time, resulting in complete degradation within 3 days. The wet weight loss of the hydrogels was reduced with increasing UV exposure time. At 120 s of UV exposure time, the wet weight remaining ratio of Ch/LA (1:1) remained unchanged during 3 days of the incubation. Ch/LA (1:1) completely degraded by 9 days. The other groups also showed significant decrease in the wet weight ($p < 0.05$), but they remained approximately 14% for Ch/LA (8:1) and Ch/LA (4:1) and 23% for the Ch alone during 15 days. At 300 s of UV exposure time, all the groups showed significant weight loss with time, but they remained approximately between 38% for Ch/LA (1:1) and 53% for the Ch alone during 15 days. Higher ratio of Ch to LA, and longer UV exposure time pronouncedly decreased wet weight remaining ratios and decelerated degradation rates.

In vitro release study

We investigated whether different ratio of Ch to LA and UV crosslinking time affects the release rate of the entrapped proteins *in vitro*. The percent cumulative release rate of BSA was measured as a function of time (Figure 6). The result showed initial burst releases of proteins from all the hydrogels followed by sustained releases at both 30 s and 300 s of UV irradiation. For 30 s of UV exposure, all the groups showed initial burst of 53–58% of the total amount within 1 day followed by slow releases of 81–91% of the total amount over 15 days of incubation. In contrast, for 300 s of UV exposure, the BSA release profile from the hydrogels yielded initial burst of 31–33% within 1 day. Subsequently, there were moderate and sustained releases of 65–74% over 15 days. Increasing UV exposure time resulted in

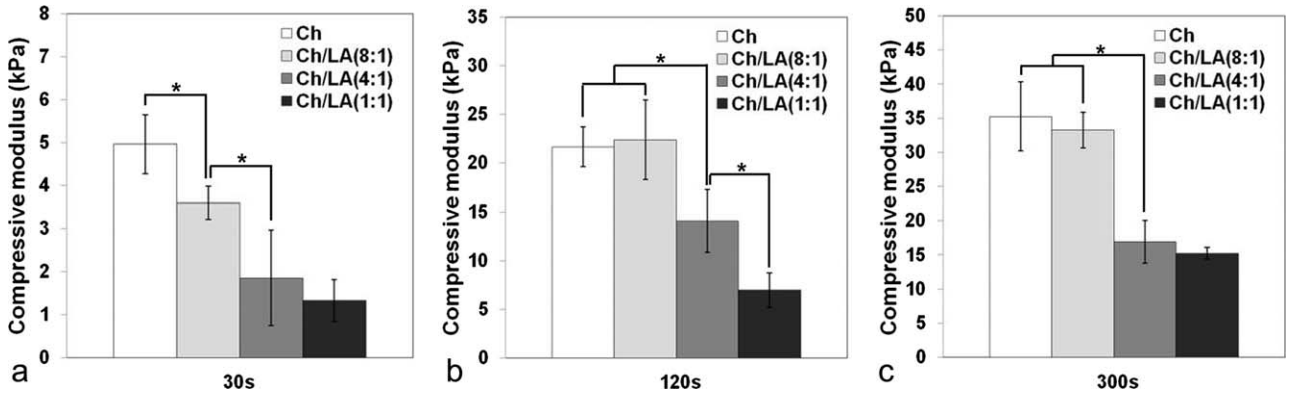

FIGURE 4. Compressive modulus of hydrogels with different ratios of Ch to LA. The prepolymer solution was exposed to 6.9 mW/cm^2 UV light for (a) 30 s; (b) 120 s; (c) 300 s. Unconfined compression tests were performed using an Instron 5944 materials testing system fitted with a 10 N load cell. The compressive modulus was determined for strain ranges of 10–20% from linear curve fits of the stress–strain curve. Each value represents the mean ± SD ($n = 3$). *Denotes significant difference between groups at same UV exposure time ($p < 0.05$).

reduced initial burst releases and extended the release periods of BSA. This study demonstrated that the release kinetics of BSA from the hydrogels was more significantly affected by UV crosslinking time than the ratios of Ch to LA over 15 days of incubation.

Cytotoxicity of hydrogels

The cytotoxicity of the hydrogels on W-20-17 and C2C12 cells was examined by a MTS assay, and the cell morphology was observed (Figure 7) for 3 days of incubation. There were significant increases in metabolic activities of W-20-17

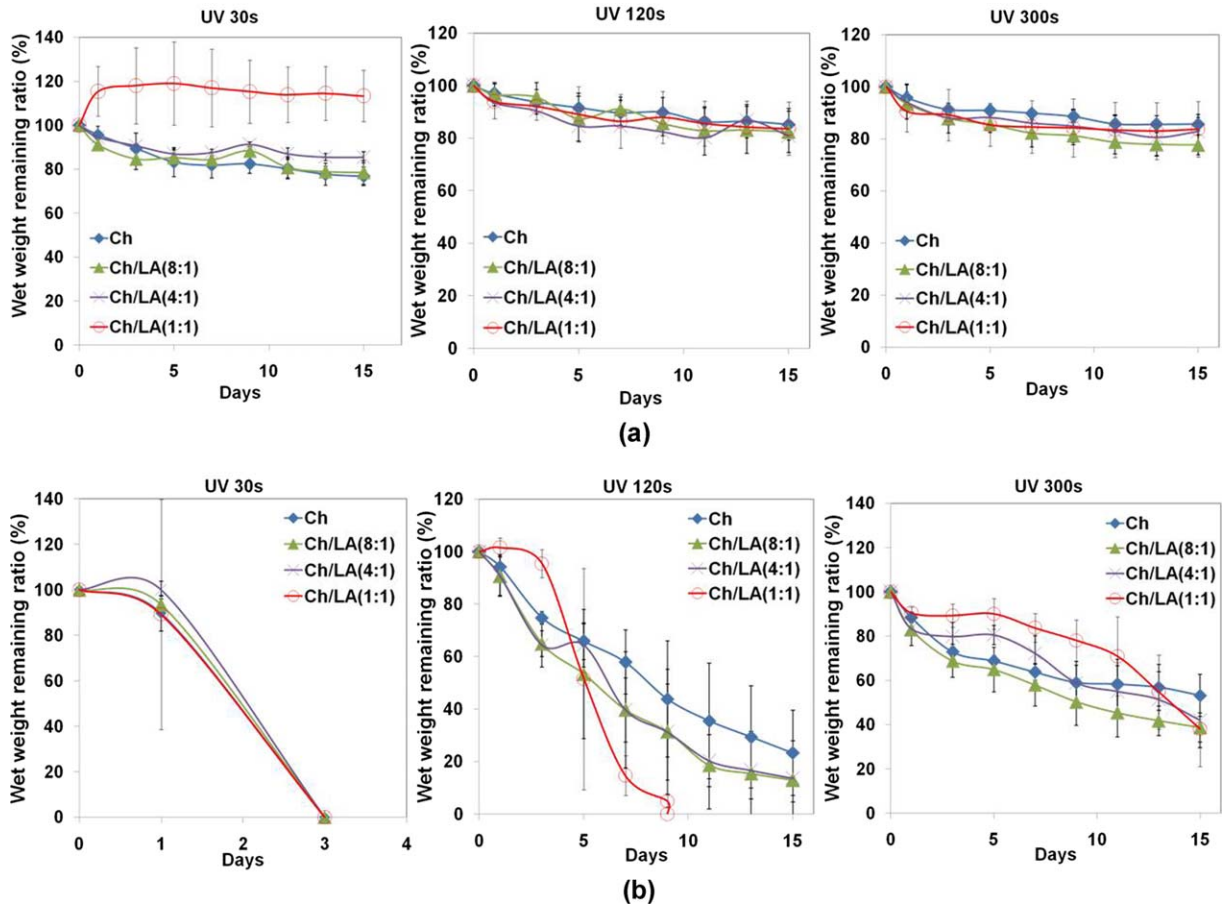

FIGURE 5. *In vitro* degradation of hydrogels in (a) PBS (pH 7.4); (b) PBS (pH 7.4) containing lysozyme (100 μg/mL) at 37°C for 15 days. The degradation profile of the hydrogels was determined by measuring the wet weight remaining ratio of the hydrogels at each time point. Each value represents the mean ± SD ($n = 4$). [Color figure can be viewed in the online issue, which is available at wileyonlinelibrary.com.]

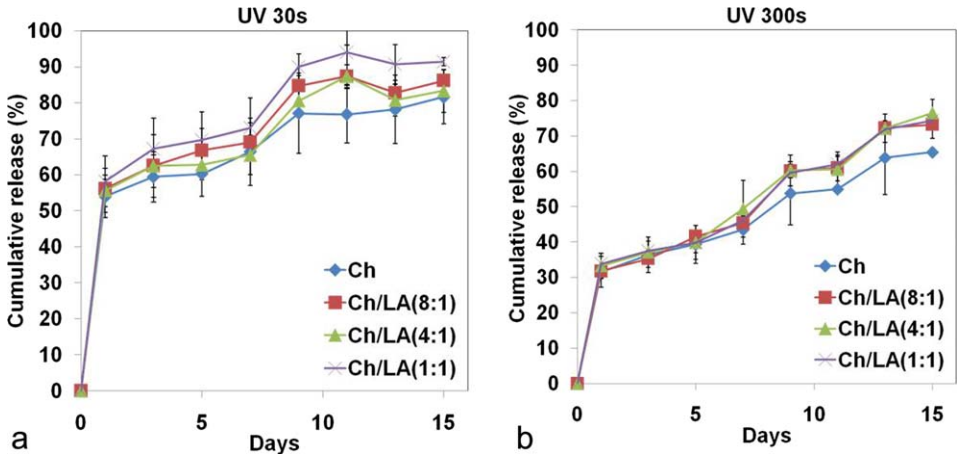

FIGURE 6. *In vitro* cumulative release profiles of bovine serum albumin (BSA) from the Ch-LA hydrogels over 15 days of incubation. BSA was directly loaded into prepolymer solution to form a homogenous solution, and then exposed to 6.9 mW/cm^2 UV light for (a) 30 s and (b) 300 s. The cumulative amounts of released BSA from the hydrogels were determined as a function of time by BCA assay at 560 nm. Each value represents the mean ± SD ($n = 3$). [Color figure can be viewed in the online issue, which is available at wileyonlinelibrary.com.]

and C2C12 cells after 3 days of culture ($p < 0.05$), indicating that the cells were viable and proliferating in the presence of the hydrogels. Consistent with the MTS assay, microscopic imaging showed that cells in all the groups significantly proliferated for 3 days of culture. Results demonstrated that the hydrogels were not cytotoxic regardless of the composition of the polymers and UV crosslinking time.

ALP activity in response to BMP-2

ALP activity of cells was measured to examine the bioactivity of BMP-2 released from the Ch/LA (8:1) hydrogels. W-20-17 and C2C12 cells were treated with BMP-2 at day 1, and their ALP activities were determined at day 5. Figure 8(a) show ALP activity of W-20-17 at different conditions. Within 5 days of cell culture, ALP activity was considerably increased with BMP-2 treatment in all the groups compared to negative control ($p < 0.05$). W-20-17 treated with BMP-2 via the hydrogel (UV 30s) expressed significantly higher ALP activity compared with the positive control ($p < 0.05$). However, there was no significant difference between hydrogels (UV 30 s and 300 s).

As shown in Figure 8(b), C2C12 also exhibited significantly lower ALP expression in negative control compared with the other groups ($p < 0.05$). C2C12 treated with BMP-2 via the hydrogel (UV 30 s) expressed the highest ALP activity during 5 days of cell culture, which was significantly greater than those of positive control and the hydrogel (UV 300 s). However, there was no significant difference between positive control and the hydrogel (UV 300 s). The results indicated that the continuous supply of BMP-2 via the photocrosslinkable hydrogels significantly affected osteoblastic differentiation of W-20-17 and C2C12.

Mineralization stained by Alizarin red S

The effects of BMP-2 treatment on mineralization and nodule formation in W-20-17 and C2C12 cells were evaluated by Alizarin Red S staining. Figure 9(a,b) shows the staining images of calcium mineral deposition of W-20-17 and C2C12 at days 10 and 21, and Figure 9(c,d) shows the analysis results. In the culture of W-20-17 [Figure 9(a)], the negative control showed no positive Alizarin Red staining at day 10 and very little staining with a small number of mineralized bone nodules at day 21. However, in the presence of BMP-2, Alizarin Red staining was pronounced in both positive control and the cultures treated with the hydrogels. The treatment of W-20-17 with BMP-2, in combination of osteogenic media, resulted in stimulation of calcium mineralization and nodule formation. The analysis results in Figure 9(c) were consistent with the visual observation in Figure 9(a). Alizarin Red S staining was significantly increased in cultures with BMP-2 at day 21 compared to day 10 ($p < 0.05$). The highest calcium accumulation occurred in both positive control and the cultures treated with the hydrogels (UV 30 s) at 21 days.

In C2C12 cultures [Figure 9(b,d)], calcium mineral formation in all groups significantly increased at day 21 compared with day 10 ($p < 0.05$). In the control groups, calcium deposition increased in a time-dependent manner, but there was no significant difference between negative and positive control groups. A significant increase in calcium mineral content was observed in the hydrogel groups compared with the control groups at day 21 ($p < 0.05$). The highest calcium accumulation was observed in cultures treated with the hydrogels (UV 300 s) at 21 days. The quantitative measurement of cell mineralization demonstrated that continuous supplemental BMP-2 to C2C12 cells via the hydrogels significantly enhanced the level of calcium deposition.

DISCUSSION

BMP-2 has been used in clinics, but the controversy on efficacy and effectiveness of high dosage BMP-2 increasingly demands the development of an ideal carrier of BMP-2.[21–23] Hydrogels have shown great promise for delivery of growth factors such as BMP-2 to guide cell functions and promote tissue integration and regeneration.[1–3] In the present study,

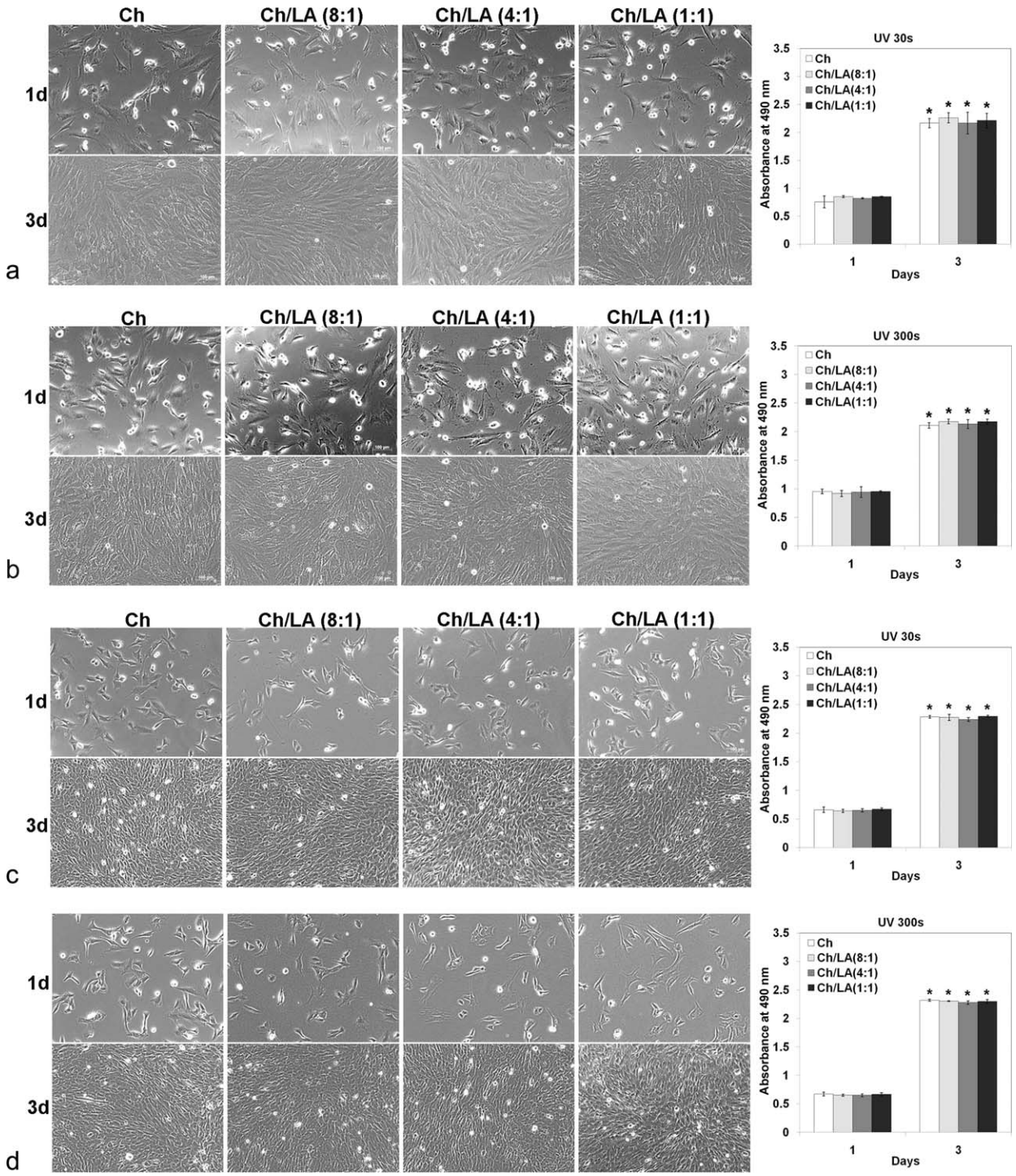

FIGURE 7. Cytotoxicity of the hydrogels via an MTS assay. Viability of W-20-17 using (a) 30 s UV; (b) 300 s UV and Viability of C2C12 using (c) 30 s UV; (d) 300 s UV. The cells were seeded at a density of 60,000 cells/well in the bottom of well plates and the hydrogels were placed into the upper chamber with culture medium. After incubation for 1 and 3 days, the number of viable cells was determined qualitatively and quantitatively (MAG = 10×). Each value represents the mean ± SD ($n = 3$). *Denotes significant difference compared with 1 day of culture ($p < 0.05$).

we synthesized and characterized a novel photo-crosslinkable, biodegradable Ch-LA hydrogel, and used this hydrogel to deliver BMP-2 to promote osteoblastic differentiation and mineralization *in vitro*.

First, the Ch-LA hydrogels were synthesized by adding D,L-lactide onto Ch, followed by methacrylation to form photo-crosslinkable copolymer networks. The chemical and structural changes of Ch, Ch/LA, and Ch/LA/MA were characterized by ^{1}H-NMR and FTIR spectra. We found that carbonyl groups of the LA interacted with hydroxyl and amine groups of the Ch. MA also reacted with the Ch-LA via the esterification and amidation. Compared to Ch/MA, Ch/LA/

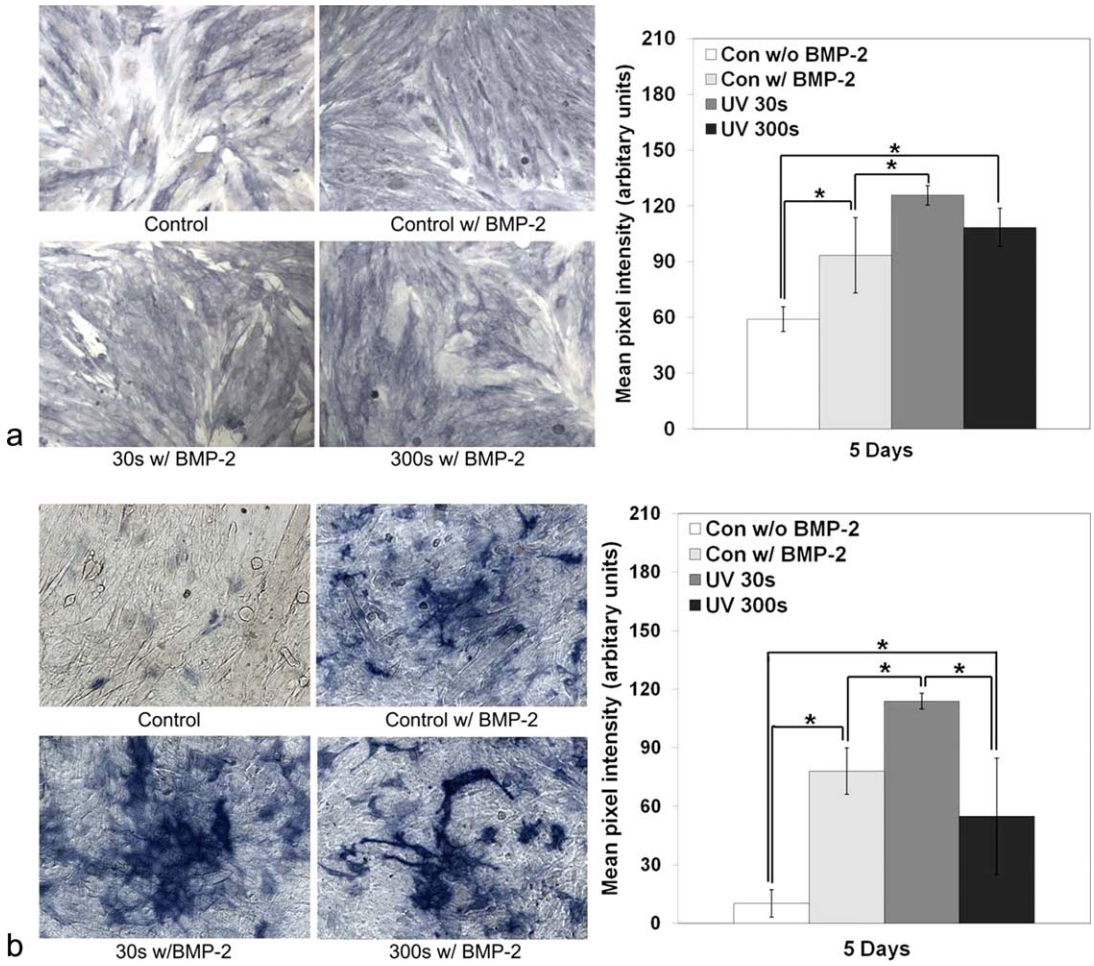

FIGURE 8. Effect of BMP-2 released from the Ch/LA (8:1) hydrogels on ALP activity of (a) W-20-17 and (b) C2C12 cells. The cells were seeded in 24-well plates at a density of 60,000 cells/well and cultured for 5 days. ALP activity was detected using Sigma-Aldrich Alkaline Phosphatase kits. Histochemical semi-quantitative imaging of ALP was obtained using a microscope. Quantification of the staining was performed using Adobe Photoshop 7.0. The image histogram tool was used to measure average pixel intensity. (MAG = 10×). Each value represents the mean ± SD ($n = 3$). *Denotes significant difference between groups ($p < 0.05$). [Color figure can be viewed in the online issue, which is available at wileyonlinelibrary.com.]

MA exhibited significantly greater degree of substitution of Ch (Supporting Information Table S1). Wu et al. reported that the amount of branched polymer increased with an increase in LA content in the feeding ratio.[11–13] Liu et al., however, demonstrated that the original integrity of Ch was disrupted when the Ch was grafted with PLA.[11] As suggested in the degree of substitution data, this is likely due to disruption of the hydrogen bonds in the Ch to a certain extent when hydroxyl and amino groups of Ch are substituted with alkyl groups of LA, resulting in a decrease in intermolecular interaction. In contrast, amide or ester linkages used for the PLA chain branches can function as plasticizers internally in the rigid main chain of Ch.[11,12] Therefore, introduction of hydrophobic LA side chains to a hydrophilic Ch backbone as well as incorporation of methacrylate will regulate the copolymer networks and interaction mechanisms, allowing for manipulation of the physicochemical properties of the copolymer.[13]

Second, the structural changes of hydrogels observed by SEM were due to the different composition of the hydrogels and crosslinking density induced by UV irradiation. Mean pore size of Ch alone was 94.5 ± 8.31 and 82.8 ± 2.43 μm at 30 s and 300 s of UV exposure time, respectively. Ch/LA (1:1) showed 576.69 ± 4.52 and 280.68 ± 30.15 μm at 30 s and 300 s, respectively. The lesser LA component, and the longer UV radiation time led to a relatively more compact network, denser surface texture, and smaller pore sizes in the Ch-LA hydrogels. The ability to control the structural changes of hydrogels can have a beneficial effect on cell signaling and communication as well as diffusion of nutrients and oxygen for bone tissue engineering applications.[2] The mechanical property of the hydrogels was consistent with the features of porous network structures. Regardless of UV radiation time, the increased amount of LA decreased the compressive modulus of the hydrogels. This is probably because PLA chain branches between crosslinks disrupted the crystalline structure of Ch evidenced by the increasing degrees of substitution. Regardless of the Ch to LA ratios, a longer UV radiation led to greater moduli of hydrogels. This is likely due to a greater degree of crosslinking via UV radiation.

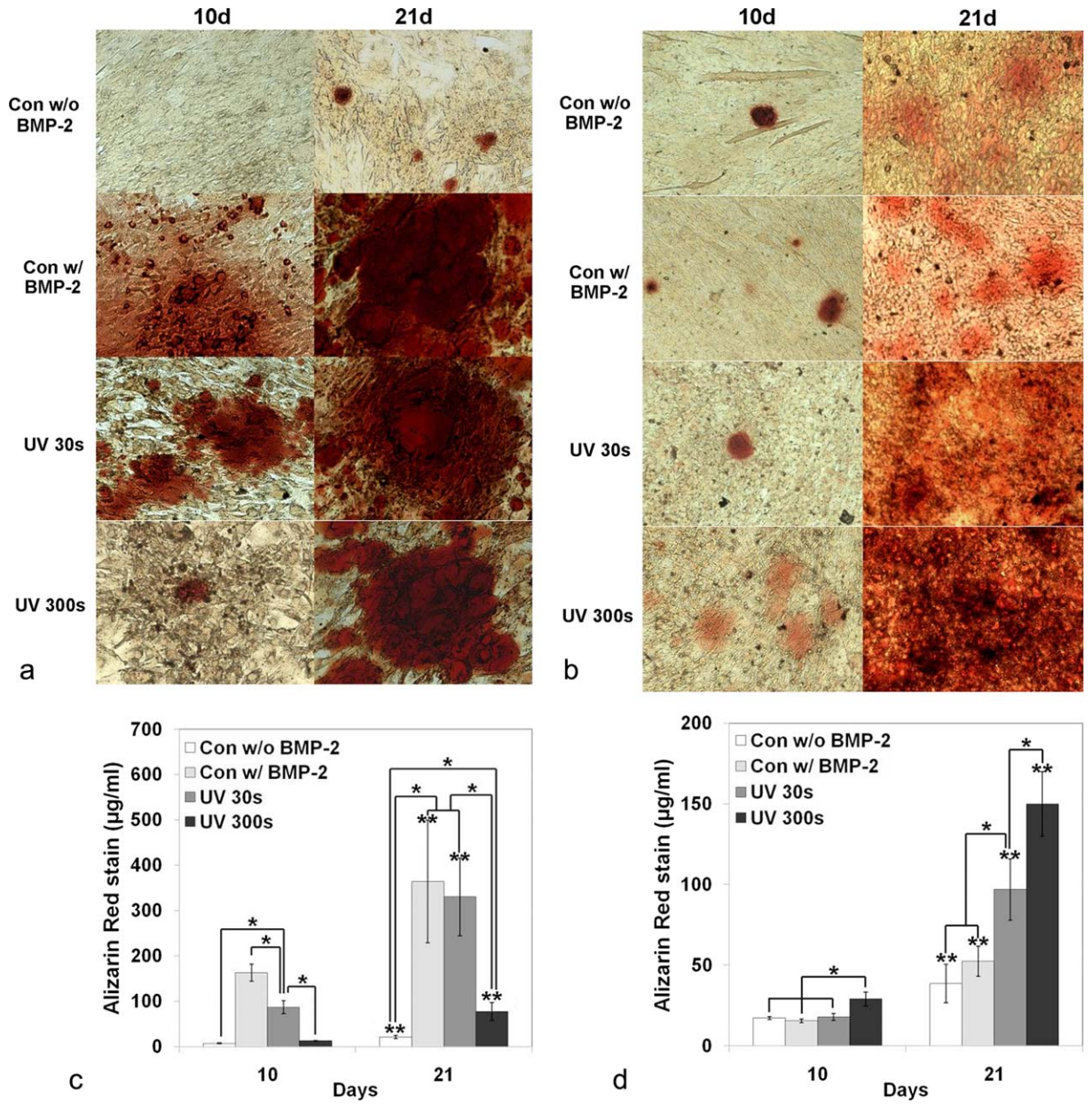

FIGURE 9. The effect of BMP-2 on calcium mineral deposition in (a) W-20-17 and (b) C2C12 cells. The presence of mineral within the cell layers was stained with Alizarin Red S staining solution at day 10 and 21. The red areas and nodules demonstrate AR-S positive staining for calcium mineral in the cell layers (MAG 10×). The calcium mineral contents quantitatively determined from Alizarin Red S staining extracts from the cell layers of (c) W-20-17 and (d) C2C12 cells at day 10 and 21. Destained Alizarin Red S concentrations were determined at the absorbance of 405 nm and expressed as μg/mL. Each value represents the mean ± SD ($n = 3$). *Denotes significant difference between groups at the same time point ($p < 0.05$). **Denotes significant difference compared with those at 10 day of culture ($p < 0.05$). [Color figure can be viewed in the online issue, which is available at wileyonlinelibrary.com.]

We also characterized the swelling behavior and degradation profile of the hydrogels by examining the wet weight remaining ratios that allows us to examine the change of the same sample over time.[4,24–27] In our study, different ratios of Ch to LA significantly affected swelling, shrinking, and enzymatic degradation of the hydrogels. The hydrogel network is connected and maintained by alkyl chains via C═C polymerization. When the hydrogel contains more PLA chain branches along the Ch main chains such as Ch/LA (1:1), the mobility and spacing of the hydrogel chains is increased.[11,12] Consequently, this will allow the hydrogel to enlarge its lattice size for absorbing and holding greater amount of water. This explains distinct swelling behavior of Ch/LA (1:1) at UV 30 s in PBS compared to other groups. As a result, the greater amount of water may increase the hydrolytic susceptibility of the hydrogel network,[10,11,17,18] and breaking the amide and ester bonds of grafted PLA.[10,18] In addition to aqueous hydrolysis, Ch, a cationic natural biopolymer, can be enzymatically degraded via Ch or lysozyme.[19,28,29] Chitosanase is absent in mammals, but

lysozyme is present and responsible for the degradation of Ch in human body. The fraction of *N*-acetylglucosamine (NAG) units in Ch contributes to its enzymatic hydrolysis.[25] The lysozyme/PBS solution significantly accelerated degradation rates of the hydrogels compared with those in absence of lysozyme. However, we have demonstrated that the enzymatic degradation rate of the hydrogels was tunable by the amount of LA in the hydrogels and the degree of crosslinking. This is likely that the higher crosslinking degree inhibited the access of lysozyme to the NAG units on the Ch chains as well as the amide and ester bonds of the hydrogel networks.[9,26] Interestingly, the fact that no change in weight ratio of the hydrogel (Ch/LA (1:1) at UV 120 s) within the first 3 days in PBS solution was probably because longer side chains of Ch/LA (1:1) could absorb greater amount of water to compensate the degradation weight loss before the hydrogel network integrity was disrupted.

These characteristics of the hydrogels are of importance in drug release kinetics via diffusion, swelling, and degradation.[21] For example, swelling of hydrogels can accelerate the diffusion of drugs by opening pores of the polymer network.[4,22,23] Surface erosion and bulk degradation of the polymers will break the polymer chains and networks, and also can accelerate the release of drugs.[21,24] In our *in vitro* release study, a model protein, BSA, was incorporated into the polymer solution and directly entrapped into the hydrogel networks after UV irradiation. The incorporation of BSA into both hydrogels via UV 30 s and UV 300 s induced a biphasic profile, including an initial burst release followed by a sustained release of BSA. The former is due to the combination effect of rapid release of proteins absorbed on the hydrogel surface and hydrogel swelling that accelerated dissolved protein diffusion.[4,22,23] The latter is regulated by the combination effect of hydrogel degradation rates and intermolecular interactions between the protein and hydrogels, including hydrogen bonding, electrostatic interactions, dipole–dipole interactions, and hydrophobic interactions.[13] We found that a higher degree of crosslinking via a longer UV irradiation significantly reduced the initial burst release and retained higher percentages of BSA loaded within the hydrogels regardless of the Ch-LA ratios.

The result of cell viability demonstrated the noncytotoxicity of the hydrogels regardless of the composition of the polymers and UV crosslinking because all formula of the hydrogels well supported cell growth and proliferation. Therefore, we continued to investigate the effect of the hydrogels (Ch/LA (8:1)) on BMP-2 induced osteoblast differentiation and mineralization. We used two cell lines as models: W-20-17 cells and C2C12 cells. Several studies demonstrated that BMP-2 induced the expression of several markers associated with the osteoblast phenotype in W-20-17 cells in a dose-dependent manner.[30–33] We also selected C2C12 cell line, which arises from the soft tissues adjacent to bone and can be reprogrammed to an osteogenic lineage via osteogenic transdifferentiation.[34–38] C2C12 myoblasts readily adopt a bone gene program in response to treatment of BMP-2.[37–39] In this study, the greater ALP activities of both W-20-17 and C2C12 cells were observed in the presence of the less crosslinked hydrogels (UV 30 s) at day 5 compared to the more crosslinked hydrogels (UV 300 s). It is most likely that the hydrogels (UV 30 s) released more BMP-2 within the time period. This result was indicated by *in vitro* model protein release profiles. In a similar study, Bhakta et al. demonstrated that BMP-2 released from hyaluronan-based hydrogels enhanced ALP activity of C2C12 in a BMP-2 dose- and time-dependent manner.[40] They found that hydrogels without heparin released more BMP-2 initially, thereby inducing a greater ALP activity of C2C12 at day 7. Findings from the studies suggest that the initial burst release of BMP-2 over the first few days significantly enhances early osteoblast differentiation. On the other hand, Kempen et al. demonstrated that the bioactivity of the BMP-2 added directly to the W-20-17 cultures was lower than that of BMP-2 delivered by composite materials, suggesting that BMP-2 is susceptible to degradation in the culture medium over a 7-day culture period.[31] Similarly, we also found that both W-20-17 and C2C12 cells expressed significantly higher ALP activities in response to a sustained BMP-2 treatment via the hydrogels (UV 30 s) compared with the positive control ($p < 0.05$).

In our mineralization study, the BMP-2 containing medium (positive control) and the hydrogels (UV 30 s) resulted in significantly higher Alizarin Red S staining and nodule formation in W-20-17 cells. The hydrogels (UV 300 s) did not enhance mineralization of W-20-17 at the early time period, but did at the later time period compared with negative control (medium without BMP-2). The results indicated that the burst release of BMP-2 significantly enhanced calcium mineralization of W-20-17. Notably, C2C12 cells produced significantly higher calcium accumulation in cultures treated with the hydrogels (UV 300 s) compared with the other groups ($p < 0.05$), including the hydrogels (UV 30 s). This is because the hydrogels (UV 300 s) probably had a slower and more release of BMP-2 at the later time period than the hydrogels (UV 30 s). Similarly, previous studies also demonstrated a continuous supplementation of BMP-2 from the delivery systems could enhance calcium mineral deposition on the layer of C2C12.[34–36,38,39] In addition, no significant difference in mineralization between negative and positive control groups indicated that initial BMP-2 treatment had no significant effect on mature bone differentiation of C2C12 cells *in vitro*, which is probably a result of no or very low expression of BMP-2 receptors on the C2C12 cells at early periods of cell incubations. This study has demonstrated that cell responses to BMP-2 are highly variable, depending on cell types, species, and different phases of phenotype maturation.[32,41,42]

Though hydrogel systems are promising in delivery of growth factors and small bioactive molecules,[1–3,8] new strategies are needed for improving local retention and sustained release of bioagents. This study was to develop and characterize Ch-LA hydrogels and test its delivery efficacy *in vitro*. Our future research would incorporate growth factor binding proteins into the hydrogels for optimization of the release kinetics of the growth factors *in vitro* and validate their delivery efficacy *in vivo*.

CONCLUSIONS

We have shown in the present study that a novel photocrosslinkable Ch-LA hydrogels can be formed via the amidation and esterification between Ch and LA, and methacrylation for further crosslinked networks. Introduction of the hydrophobic moiety of LA to Ch, and crosslinking via UV irradiation significantly affected structural and mechanical properties as well as degradation profiles of the hydrogels. The Ch-LA hydrogels effectively delivered BMP-2 to induce osteoblastic differentiation and mineralization. The advantages of this novel Ch based hydrogel are the injectable formula that can be easily applied to the target site, and tunable protein release kinetics and properties via composition and UV radiation.

REFERENCES

1. Uebersax L, Merkle HP, Meinel L. Biopolymer-based growth factor delivery for tissue repair: From natural concepts to engineered systems. Tissue Eng Part B Rev 2009;15:263–289.
2. Vo TN, Kasper FK, Mikos AG. Strategies for controlled delivery of growth factors and cells for bone regeneration. Adv Drug Deliv Rev 2012;64:1292–1309.
3. Jeon O, Powell C, Solorio LD, Krebs MD, Alsberg E. Affinity-based growth factor delivery using biodegradable, photocrosslinked heparin-alginate hydrogels. J Control Release 2011;154:258–266.
4. Pitarresi G, Casadei MA, Mandracchia D, Paolicelli P, Palumbo FS, Giammona G. Photocrosslinking of dextran and polyaspartamide derivatives: A combination suitable for colon-specific drug delivery. J Control Release 2007;119:328–338.
5. Leach JB, Schmidt CE. Characterization of protein release from photocrosslinkable hyaluronic acid-polyethylene glycol hydrogel tissue engineering scaffolds. Biomaterials 2005;26:125–135.
6. Billiet T, Vandenhaute M, Schelfhout J, Vlierberghe SV, Dubruel P. A review of trends and limitations in hydrogel-rapid prototyping for tissue engineering. Biomaterials 2012;33: 6020–6041.
7. Lee JY, Nam SH, Im SY, Park YJ, Lee YM, Seol YJ, Chung CP, Lee SJ. Enhanced bone formation by controlled growth factor delivery from chitosan-based biomaterials. J Control Release 2002;78: 187–197.
8. Tabata Y. Tissue regeneration based on growth factor release. Tissue Eng 2003;9 (Suppl 1):S5–S15.
9. Kim S, Gaber MW, Zawaski JA, Zhang F, Richardson M, Zhang XA, Yang Y. The inhibition of glioma growth in vitro and in vivo by a chitosan/ellagic acidcomposite biomaterial. Biomaterials 2009;30:4743–4751.
10. Lü S, Liu M, Ni B. An injectable oxidized carboxymethyl cellulose/N-succinyl-chitosan hydrogel system for protein delivery. Chem Eng J 2010;160:779–787.
11. Liu Y, Tian F, Hu KA. Synthesis and characterization of a brush-like copolymer of polylactide grafted onto chitosan. Carbohydr Res 2004;339:845–851.
12. Wu Y, Zheng Y, Yang W, Wang C, Hu J, Fu S. Synthesis and characterization of a novel amphiphilic chitosan–polylactide graft copolymer. Carbohydr Polym 2005;59:165–171.
13. Bhattarai N, Ramay HR, Chou SH, Zhang M. Chitosan and lactic acid-grafted chitosan nanoparticles as carriers for prolonged drug delivery. Int J Nanomed 2006;1:181–187.
14. Ivirico JLE, Salmerón-Sánchez M, Ribelles JG, Pradas MM. Poly(L-lactide) networks with tailored water sorption. Colloid Polym Sci 2009;287:671–681.
15. Yu LM, Kazazian K, Shoichet MS. Peptide surface modification of methacrylamide chitosan for neural tissue engineering applications. J Biomed Mater Res A 2007;82:243–255.
16. Radhakumary C, Nair PD, Mathew S, Nair CP. Biopolymer composite of chitosan and methyl methacrylate for medical applications. Trends Biomater Artif Organs 2005;18:117–124.
17. An J, Yuan X, Luo Q, Wang D. Preparation of chitosan-graft-(methylmethacrylate)/Ag nanocomposite with antimicrobial activity. Polym Int 2010;59:62–70.
18. Hong Y, Song H, Gong Y, Mao Z, Gao C, Shen J. Covalently crosslinked chitosan hydrogel: Properties of in vitro degradation and chondrocyte encapsulation. Acta Biomater 2007;3:23–31.
19. Porstmann B, Jung K, Schmechta H, Evers U, Pergande M, Porstmann T, Kramm HJ, Krause H. Measurement of lysozyme in human body fluids: Comparison of various enzyme immunoassay techniques and their diagnostic application. Clin Biochem 1989; 22:349–355.
20. Kowapradit J, Opanasopit P, Ngawhiranpat T, Apirakaramwong A, Rojanarata T, Ruktanonchai U, Sajomsang W. Methylated *N*-(4-*N*,*N*-dimethylaminobenzyl) chitosan, a novel chitosan derivative, enhances paracellular permeability across intestinal epithelial cells (Caco-2). AAPS Pharm Sci Technol 2008;9:1143–1152.
21. Calori GM, Donati D, Di Bella C, Tagliabue L. Bone morphogenetic proteins and tissue engineering: Future directions. Injury 2009;40: S67–S76.
22. Carragee EJ, Hurwitz EL, Weiner BK. A critical review of recombinant human bone morphogenetic protein-2 trials in spinal surgery: Emerging safety concerns and lessons learned. Spine J 2011;11:471–491.
23. Shields LB, Raque GH, Glassman SD, Campbell M, Vitaz T, Harpring J, Shields CB. Adverse effects associated with high-dose recombinant human bone morphogenetic protein-2 use in anterior cervical spine fusion. Spine 2006;31:542–547.
24. Lin CC, Metters AT. Hydrogels in controlled release formulations: Network design and mathematical modeling. Adv Drug Deliv Rev 2006;58:1379–1408.
25. Al-Kahtani Ahmed A, Bhojya Naik HS, Sherigara BS. Synthesis and characterization of chitosan-based pH-sensitive semi-interpenetrating network microspheres for controlled release of diclofenac sodium. Carbohydr Res 2009;344:699–706.
26. Guo BL, Gao QY. Preparation and properties of a pH/temperature-responsive carboxymethyl chitosan/poly(N-isopropylacrylamide) semi-IPN hydrogel for oral delivery of drugs. Carbohydr Res 2007; 342:2416–2422.
27. Siepmann J, Peppas NA. Modeling of drug release from delivery systems based on hydroxypropyl methylcellulose (HPMC). Adv Drug Deliv Rev 2001;48:139–157.
28. Stokke BT, Varum KM, Holme HK, Hjerde RJN, Smidsrod O. Sequence specificities for lysozyme depolymerization of partially N-acetylated chitosans. Can J Chem 1995;73:1972–1981.
29. Freier T, Koh HS, Kazazian K, Shoichet MS. Controlling cell adhesion and degradation of chitosan films by N-acetylation. Biomaterials 2005;26:5872–5878.
30. Thies RS, Bauduy M, Ashton BA, Kurtzberg L, Wozney JM, Rosen V. Recombinant human bone morphogenetic protein-2 induces osteoblastic differentiation in W-20-17 stromal cells. Endocrinology 1992;130:1318–1324.
31. Kempen DH, Lu L, Hefferan TE, Creemers LB, Maran A, Yaszemski MJ. Retention of in vitro and in vivo BMP-2 bioactivities in sustained delivery vehicles for bone tissue engineering. Biomaterials 2008;29:3245–3252.
32. Kim S, Tsao H, Kang Y, Young DA, Sen M, Wenke JC, Yang Y. In vitro evaluation of an injectable chitosan gel for sustained local delivery of BMP-2 for osteoblastic differentiation. J Biomed Mater Res B Appl Biomater 2011;99:380–390.
33. Nguyen AH, Kim S, Maloney WJ, Wenke JC, Yang Y. Effect of coadministration of vancomycin and BMP-2 on cocultured Staphylococcus aureus and W-20-17 mouse bone marrow stromal cells in vitro. Antimicrob Agents Chemother 2012;56: 3776–3784.
34. Liu R, Ginn SL, Lek M, North KN, Alexander IE, Little DG, Schindeler A. Myoblast sensitivity and fibroblast insensitivity to osteogenic conversion by BMP-2 correlates with the expression of Bmpr-1a. BMC Musculoskelet Disord 2009;10:1–12.
35. Bramono DS, Murali S, Rai B, Ling L, Poh WT, Lim ZX, Stein GS, Nurcombe V, van Wijnen AJ, Cool SM. Bone marrow-derived heparan sulfate potentiates the osteogenic activity of bone morphogenetic protein-2 (BMP-2). Bone 2012;50:954–964.
36. Jeong BC, Lee YS, Park YY, Bae IH, Kim DK, Koo SH, Choi HR, Kim SH, Franceschi RT, Koh JT, Choi HS. The orphan nuclear receptor estrogen receptor-related receptor gamma negatively

regulates BMP2-induced osteoblast differentiation and bone formation. J Biol Chem 2009;284:14211–14218.
37. Schindeler A, Liu R, Little DG. The contribution of different cell lineages to bone repair: Exploring a role for muscle stem cells. Differentiation 2009;77:12–18.
38. Katagiri T, Yamaguchi A, Komaki M, Abe E, Takahashi N, Ikeda T, Rosen V, Wozney JM, Fujisawa-Sehara A, Suda T. Bone morphogenetic protein-2 converts the differentiation pathway of C2C12 myoblasts into the osteoblast lineage. J Cell Biol 1994;127:1755–1766.
39. Yamaguchi A, Katagiri T, Ikeda T, Wozney JM, Rosen V, Wang EA, Kahn AJ, Suda T, Yoshiki S. Recombinant human bone morphogenetic protein-2 stimulates osteoblastic maturation and inhibits myogenic differentiation in vitro. J Cell Biol 1991;113:681–687.
40. Bhakta G, Rai B, Lim ZX, Hui JH, Stein GS, van Wijnen AJ, Nurcombe V, Prestwich GD, Cool SM. Hyaluronic acid-based hydrogels functionalized with heparin that support controlled release of bioactive BMP-2. Biomaterials 2012;33:6113–6122.
41. Diefenderfer DL, Osyczka AM, Garino JP, Leboy PS. Regulation of BMP-induced transcription in cultured human bone marrow stromal cells. J Bone Joint Surg Am 2003;85:19–28.
42. Osyczka AM, Diefenderfer DL, Bhargave G, Leboy PS. Osteogenesis versus chondrogenesis by BMP-2 and BMP-7 in adipose stem cells. Cells Tissues Organs 2004;176:109–119.